AGU PUBLICATIONS

Geophysical Research Letters

RESEARCH LETTER
10.1002/2015GL063769

Key Points:
- GRACE gravity rate shows significant signal in the Barents Sea
- Presented regional ice-loading model represents GRACE gravity rate better
- A local weaker mantle is needed to fit ICE-5G to GRACE observations

Supporting Information:
- Text S1, Figures S1–S3, and Table S1

Correspondence to:
B. C. Root,
b.c.root@tudelft.nl

Citation:
Root, B. C., L. Tarasov, and W. van der Wal (2015), GRACE gravity observations constrain Weichselian ice thickness in the Barents Sea, *Geophys. Res. Lett.*, *42*, 3313–3320, doi:10.1002/2015GL063769.

Received 6 MAR 2015
Accepted 19 APR 2015
Accepted article online 23 APR 2015
Published online 13 May 2015

GRACE gravity observations constrain Weichselian ice thickness in the Barents Sea

B. C. Root[1], L. Tarasov[2], and W. van der Wal[1]

[1]Department of Astrodynamics and Space Missions, Delft University of Technology, Delft, Netherlands, [2]Department of Physics and Physical Oceanography, Memorial University, St. John's, Newfoundland, Canada

Abstract The Barents Sea is subject to ongoing postglacial uplift since the melting of the Weichselian ice sheet that covered it. The regional ice sheet thickness history is not well known because there is only data at the periphery due to the locations of Franz Joseph Land, Svalbard, and Novaya Zemlya surrounding this paleo ice sheet. We show that the linear trend in the gravity rate derived from a decade of observations from the Gravity Recovery and Climate Experiment (GRACE) satellite mission can constrain the volume of the ice sheet after correcting for current ice melt, hydrology, and far-field gravitational effects. Regional ice-loading models based on new geologically inferred ice margin chronologies show a significantly better fit to the GRACE data than that of ICE-5G. The regional ice models contain less ice in the Barents Sea than present in ICE-5G (5–6.3 m equivalent sea level versus 8.5 m), which increases the ongoing difficulty in closing the global sea level budget at the Last Glacial Maximum.

1. Introduction

The geological sea level record in Barbados [*Peltier and Fairbanks*, 2006] estimates the sea level at the Last Glacial Maximum (LGM) to be on average 120 m lower than the present-day sea level. The widely used ICE-5G reconstruction [*Peltier*, 2004] has a total volume of LGM-grounded ice equivalent to a 118.7 m sea level rise assuming the present-day ocean area. However, since publication of the model, recent reconstructions of the Antarctic ice sheet have a smaller LGM-grounded ice volume compared to the 17.3 m eustatic sea level (ESL) of ICE-5G [*Peltier*, 2004]. These include both pure Glacial Isostatic Adjustment (GIA) reconstructions (7 mESL) [*Ivins et al.*, 2013], as well as hybrid glaciological/GIA modeling approaches (8–10 mESL) [*Whitehouse et al.*, 2012] and (6–15 mESL) [*Briggs et al.*, 2014]. Geodetic data of North America have indicated a smaller ice sheet there [*Lambert et al.*, 2006; *van der Wal et al.*, 2009; *Argus and Peltier*, 2010] as also occurs in a recent data-calibrated glaciological reconstruction [*Tarasov et al.*, 2012]. *Clark and Tarasov* [2014] suggest previously unaccounted for grounded ice in the Northern Hemisphere as solution for missing LGM ice. To exacerbate the problem, a revision of the GIA model to reflect the effect of a high-viscosity slab in the mantle below Barbados brings the sea level rise inferred from Barbados to about 130 m [*Austermann et al.*, 2013]. Thus, the total ice volume required to match sea level data is increased, while the contribution from the known ice sheets in North America and Antarctica is smaller than previously thought. The missing ice must come from other ice sheets of which the thickness is not well constrained yet.

One possibility to locate some of the missing ice is the Barents Sea region, which delivers 8.5 m of sea level rise in the ICE-5G model. This area is one of the largest continental shelves, which could have been completely ice covered during the LGM [*Svendsen et al.*, 2004]. However, the ice cover during the LGM in this area is heavily debated, with some stating that large parts of the northern coastal areas of Russia were covered with ice sheets [*Grosswald*, 1998]. Furthermore, sea level curves collected from the coasts of Svalbard, Novaya Zemlya, and Franz Joseph Land indicate grounded ice in the Barents Sea region at the LGM [*Kaufmann*, 1997]. Others argue that the ice margin during the LGM was situated offshore, covering only the northern tip of the Taymyr Peninsula [*Mangerud et al.*, 2002; *Lambeck*, 1996]. Unfortunately, all these studies could only use observations that are located at the boundaries of the predicted postglacial uplift, probing areas far away from the maximum expected uplift. Observations in the center of the Barents Sea (see Figure 1) could reduce the uncertainty of LGM ice mass estimates and contribute to resolving the global ice budget of land ice at the LGM.

Observations of time-variable gravity from the GRACE satellite mission have been able to constrain ice-loading history in North America [*Tamisiea et al.*, 2007] and are successfully used in Scandinavia [*Steffen et al.*, 2008;

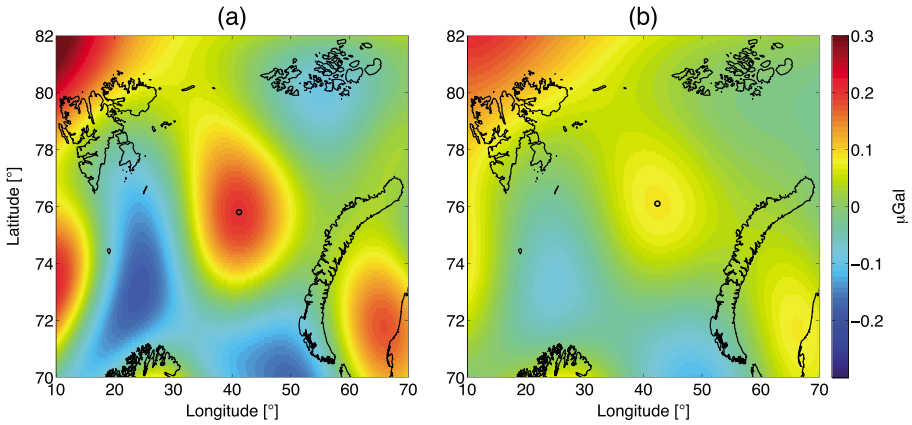

Figure 1. Gravity Recovery and Climate Experiment (GRACE) gravity trends at the surface after band-pass filtering and correction for present-day ice mass change. A band-pass filter with high-pass half width of (a) 200 km and (b) 300 km and low-pass half width of 600 km for both models is assumed. The present-day ice mass change corrections adopted are −3.3 Gt/yr (Svalbard), −4.2 Gt/yr (Novaya Zemlya), and −0.9 Gt/yr (Franz Joseph Land). The black dot depicts the location of maximum gravity change.

Root et al., 2015]. The gravity rate in areas of uplift in North America and Scandinavia was shown to agree with uplift rates measured by GPS uplift rates [*van der Wal et al.*, 2011]. With the increased precision of later GRACE releases and longer observational time series, signals of smaller spatial scale should become more visible against background noise. This study investigates the constraint provided by GRACE data on models of the past ice sheet in the Barents Sea. We compare the GRACE-derived gravity rate with the predicted gravity rate from GIA models with different mantle parameters and for different ice-loading histories, assessing whether or not the employed ice-loading models are a good representation of the past ice thickness at the Barents Sea region.

2. Ice-Loading Models

The regional ice sheet chronologies are from an ongoing Bayesian calibration of the glaciological Glacial Systems Model (GSM) for Northern Europe and adjacent continental shelves. The Bayesian calibration follows the approach of *Tarasov et al.* [2012] and thereby generates a posterior probability distribution of ice sheet chronologies given GSM run fits to the calibration constraints. The latter consists of Relative Sea Level (RSL) data, present-day vertical velocities, and a geologically inferred deglacial ice margin chronology (DATED) [*Hughes et al.*, 2014]. The RSL data are from a slightly cleaned up 2006 snapshot of the University of Toronto database upon which ICE-5G was based [*Peltier*, 2004]. The ice margin chronology is distinguished by the inclusion of inferred maximum/minimum ice margin isochrones for each time slice. This DATED chronology was recently revised, and we include results from calibrations with both the older and newer versions of DATED, which had, respectively, later ("late deglaciation models") and earlier ("early deglaciation models") deglaciation of the Barents Sea region. The initial calibration used uplift data from *Argus and Peltier* [2010], while the revised calibration with the newer version of DATED also used an updated and much larger set of geodetic constraints from *Kierulf et al.* [2014].

The selected regional ice-loading models, which have a low misfit to the RSL and uplift data, are compared to the ice thicknesses of the global ice-loading model, ICE-5G [*Peltier*, 2004]. We use ICE-5G version 1.2 with an order 256 Gaussian grid for the complete time period of 0–122 ka, downloaded from http://www.atmosp.physics.utoronto.ca/~peltier/data.php. In the case of the regional ice sheet models, the North Eurasian ice sheets in ICE-5G were replaced by the calibrated ice sheets. ICE-6G ice thickness values are not available, we therefore use the published Stokes coefficients for ICE-6G_C (VM5a), see Figures 2a and 2b. The latest Australian National University model [*Schmidt et al.*, 2014] is outdated, and a new model will be published soon (K. Lambeck, personal communication, 2015), so it is not used in this study.

The ice volume equivalent sea level for the different ice models for the Barents Sea region used in this study can be seen in Figures 2c and 2d. The selected regional models all have low misfit values to the RSL and GPS uplift data sets. The ESL change for the Barents Sea is a numerical conversion of the ice volume change

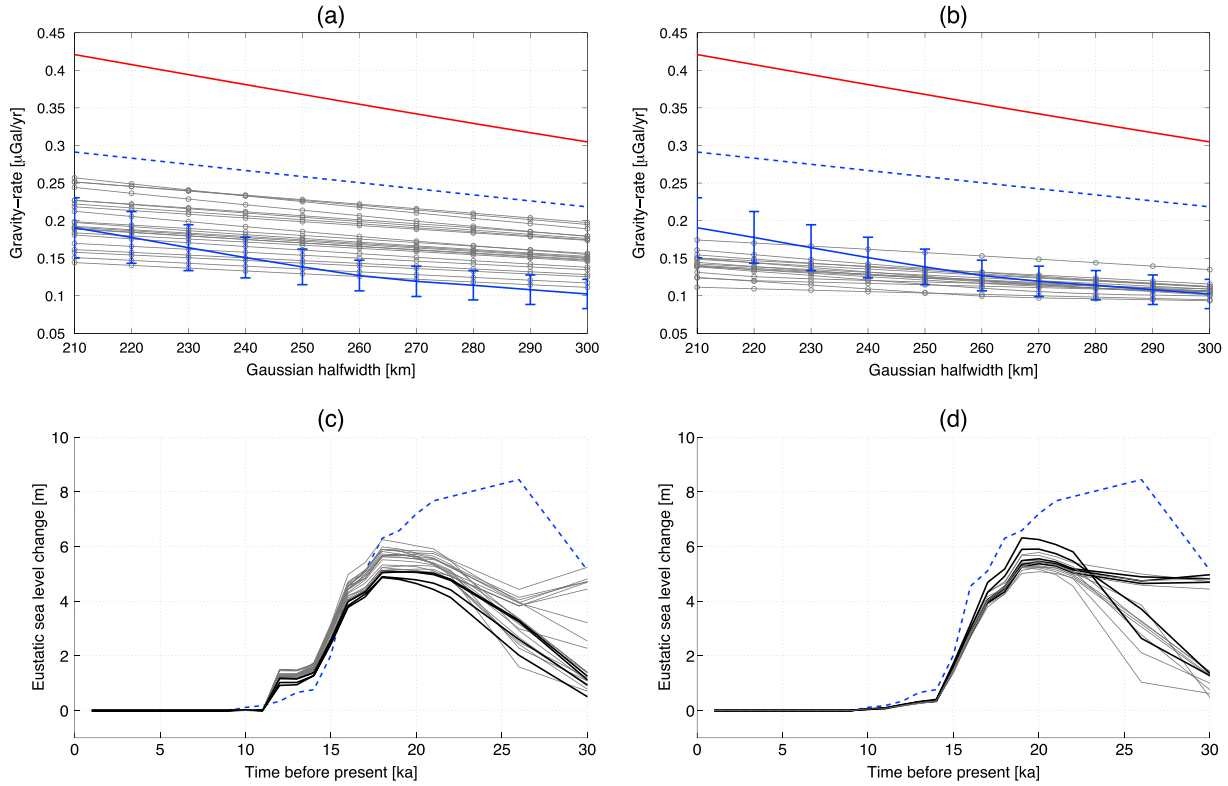

Figure 2. (a and b) Maximum gravity rate in the Barents Sea. The solid blue line depicts the GRACE observations with the error bar indicating the uncertainty in ice mass loss estimates from Table 1 and the formal errors. The dashed blue line shows the GIA model results using ICE-5G, the red represents ICE-6G. The spread in maximum gravity rate of the *Tarasov et al.* [2012] models are shown (grey) for late deglaciation (Figure 2a) and early deglaciation (Figure 2b). On the *x* axis are different low-pass filter half widths. The high-pass filter half width is set to 600 km for this particular representation. (c and d) The ice volumes of the different models expressed as equivalent sea level change. The dashed blue line is the ICE-5G model. Regional models with late deglaciation (Figure 2c). Regional models with early deglaciation (Figure 2d). The grey lines represent ice-loading models that failed the GRACE criteria, and the solid black lines passes this criteria.

above 69° latitude and between 0° and 60° longitude, using a density ice and liquid water to be 920 kg/m^3 and 1000 kg/m^3, respectively. The contribution from the grounded ice in the Barents Sea region ranges from 8.5 m (ICE-5G) to 5–6.3 m (DATED models). The older late deglaciation-calibrated ice models have a similar onset of glaciation as the ICE-5G model.

3. GIA Model

In GIA modeling, the surface load consists of land ice and water redistribution. These are obtained by solving the full sea level equation, including meltwater influx, time-dependent continent margins, and rotational feedback [*Mitrovica and Peltier*, 1991], [*Kendall et al.*, 2005]. The response of the solid Earth to a surface load is computed using the multilayered normal-mode method [*Wu and Peltier*, 1982; *Vermeersen and Sabadini*, 1997]. Full details can be found in *van der Wal et al.* [2009]. To see the effect of the different ice-loading histories on the gravity change, similar rheological models for the Earth layers are used. The model consists of an elastic lithosphere of 60 km, followed by a 40 km thin sublithospheric layer with a viscosity of 1×10^{22} Pa s, an upper mantle (570 km) with a viscosity of 0.5×10^{21} Pa s, and a double layered lower mantle with viscosities of 1.6×10^{21} (500 km) and 3.2×10^{21} (1720 km). This viscosity structure is called VM5a [*Peltier and Drummond*, 2008]. Later, the rheological parameters will be varied to study their effect on gravity change estimation in the Barents Sea.

To evaluate the different models, a misfit criterion is defined [*Press et al.*, 1992]

$$\chi^2 = \frac{1}{N_i}\sum_i \left(\frac{o_i - m_i}{s_i}\right)^2, \quad (1)$$

where the corrected GRACE observations are represented by *o*, with the standard deviation expressed in *s*. The GIA model results are represented by *m*, and the subscript *i* represent different filter settings to the GRACE

Table 1. The Ice Mass Loss Estimates From GRACE Based on a Global Mascon Solution Compared to Results From Literature[a]

Location	Area (km^2)	Estimate (Gt/yr)	Jacob et al. (2012) (Gt/yr)	Estimate (Gt/yr)	Moholdt et al. (both) (Gt/yr)
Svalbard	56,400	−3.3 ±1.2	−3 ±2	−4.8 ± 0.3	−4.3 ± 1.4
Novaya Zemlya	47,600	−4.2 ±1.0	−4 ±2	−8.0 ± 0.3	−7.6 ± 1.2
Franz J. Land	16,150	−0.9 ±0.7	0 ±2	−1.9 ± 0.6	−0.9 ± 0.7
Total:	120,150	−8.4 ±1.7	−7 ±3.5	14.7 ± 0.73	−12.8 ± 2.0
				ICESat period	(2003–2008)

[a]The study of *Jacob et al.* [2012] also uses a global mascon model, and *Moholdt et al.* [2010, 2012] is based on ICESat altimetry data of the melting ice sheets.

data (see supporting information). *N* is the number of data points, which reflects the number of different filter settings of the GRACE data.

4. GRACE Data

The GRACE observations used in this study are the CSR Release 5 monthly gravity fields [*Bettadpur*, 2003] for the period February 2003 up to and including July 2013. The degree 2, order 0 coefficients are replaced by the values from Satellite Laser Ranging [*Cheng et al.*, 2013]. A linear trend is estimated in the presence of an annual and semiannual signal. In the Barents Sea, these linear-trend gravity solutions contain the gravity change due to GIA as well as ongoing ice melt, continental water storage changes, and noise.

Ice mass loss in the Arctic Archipelagos of the Barents Sea can be estimated independently from GRACE with data from the ICESat mission [*Moholdt et al.*, 2010, 2012; *Nuth et al.*, 2010], but it stopped operating after 2008. Therefore, in this study, we employ mass loss rate estimates from GRACE based on a global mascon model [*Schrama et al.*, 2014] (Table 1). Mass loss estimates need to be corrected for GIA effects. The correction introduces an uncertainty, however, this is small compared to other systematic errors in the mass loss estimation. To validate, the values from the mascon solution are compared with those of *Jacob et al.* [2012] and they overlap within uncertainties. Furthermore, the solutions agree within the uncertainty with the estimates in the ICESat-based studies of *Moholdt et al.* [2010] and *Moholdt et al.* [2012] for the period of 2003–2008 (see Table 1).

To correct the GRACE data for ongoing glacial mass changes, the areal extent of the ice melt is required in addition to the mass loss estimates. The ice mass losses are homogeneously distributed over the glaciated areas of Svalbard (approximated melt area of 56,400 km^2), Franz Joseph Land (approximated melt area is 16,150 km^2), and Novaya Zemlya (approximated melt area is 47,600 km^2) north of 73° latitude. The ice mass losses in Table 1 are converted to surface mass changes and subsequently converted to gravitational potential coefficients taking into account elastic loading [*Wahr et al.*, 1998].

Finally, continental water storage changes are corrected for using the Global Land Data Assimilation System (GLDAS) model [*Rodell et al.*, 2004] from which glaciated areas were excluded. A Gaussian band-pass filter is used to reduce remaining noise in the GRACE observations. However, too much filtering removes a substantial part of the GIA signal while too little leaves noise in the data. In the supporting information, we show that our conclusion is valid for a range of Gaussian low-pass filter half widths between 200 km and 300 km. Long wavelength signals from other sources, such as the ice mass changes in Greenland and continental hydrology uncorrected for by the GLDAS model, can be mitigated by removing the low degrees in the GRACE data and GIA models, using a high-pass Gaussian filter, varying the half widths between 500 and 700 km. Effects of internal dynamics of the deep Earth are also filtered, but we reckon that this motion is not fast enough to be observed by GRACE. *Greff-Lefftz et al.* [2010] showed that no visible effect is seen in the $\dot{J}_2$ coefficient.

The corrected GRACE data show a positive gravity anomaly rate in the area where postglacial rebound is expected. We use the maximum value of that signal to compare with the GIA models. Several factors contribute to the uncertainty in the observed gravity rate in the center of the Barents Sea. Formal errors in the GRACE data are estimated assuming that the geophysical signals are explained by an annual signal, a semiannual signal, and a trend [*Wahr et al.*, 2004]. The residuals are upscaled to account for the reduction in noise after removing a trend and annual signal from a random time series. Systematic errors result from error in

the present-day ice melt estimates including the GIA correction. Assuming that the formal errors are independent from the systematic errors, uncertainty components are added in quadrature to obtain the total uncertainty estimate for the GRACE-derived GIA gravity rate. The total (2σ) uncertainty in the GRACE gravity change observations is shown as error bars in Figures 2a and 2b.

5. Results

In Figures 2a and 2b, the maximum gravity rates from the different GIA models are compared with the maximum gravity rate derived from the corrected GRACE observation for different settings of the band-pass filter. The GRACE-derived gravity rate is smaller than the GIA model result using ICE-5G and ICE-6G. The regional ice models with the late deglaciation chronology mostly overestimate the GRACE-derived maximum gravity rate in the Barents Sea region. Only four of the late deglaciation models fall completely within the uncertainty of the GRACE observations, irrespective of the filter settings. Many of the early deglaciation models pass the GRACE gravity rate criterion. However, some tend to underestimate the gravity rate in the region. Misfit with respect to RSL, GPS uplift, and GRACE observations per individual ice model is shown in the supporting information.

To examine which characteristics of the ice model cause mismatches with the GRACE-derived gravity rate, Figures 2c and 2d illustrate the ESL through time for the different models. The overestimation in the late deglaciation ice models (including ICE-5G) is a combination between time of melting and the overall ice mass in the region. Only models that have no more than 5.1 mESL during 18–21 ka pass the GRACE criteria: nn43772, nn44901, nn45283, and nn96597 (see supporting information for numbering). The ice models that fit the GRACE data have less than 4 mESL ice volume at 16 ka and have relative small ice volumes during the 20–30 ka interval.

The early deglaciation models have a tendency to underestimate the gravity change. As a result of the earlier deglaciation onset, these models can have more ice volume during the LGM while maintaining consistency with GRACE. The model nn54867 has an ice volume of more than 6.2 mESL at 20 ka and still fits the GRACE data. Additionally, early deglaciation models that pass the GRACE criterion have at least 5.2 mESL of ice at LGM.

Early deglaciation models that have ice volume continuously above 4 mESL during the 20-30 ka period show a different behavior. By inspecting Figure 2d, a small number of the lowest ice volume early deglaciation models pass the criterion. Model nn55917 does not pass the criterion even though it has less ice (5.78 mESL) than the early deglaciation model with the most ice mass during LGM. Finally, ICE-6G is also an early deglaciation model, but has thick ice in the Barents Sea region around 30 ka, which explains the large overestimation of the gravity change. This suggests that GRACE is sensitive to ice mass change in the 20–30 ka period.

To further asses the constraint to GIA modeling provided by the GRACE data in the Barents Sea, we examine how much the rheology should change, such that the ice models become acceptable. The upper mantle viscosity is varied from 2, 4, 8, 16 to 32 $\times 10^{20}$ Pa s. The lithosphere thickness is varied between 40 and 160 km with a step size of 20 km. The size of the Barents Sea ice sheet is too small for the uplift to be sensitive to the lower mantle viscosity [*Steffen and Kaufmann*, 2005]; therefore, we keep this parameter fixed at 32×10^{20} Pa s to approximate the VM5a structure.

Figure 3 shows the misfit results for the following ice models: ICE-5G, two late deglaciation models (minimum and maximum overall ice mass), two early deglaciation models (minimum and maximum overall ice mass), and a third early deglaciation ice model with large amount of ice (more than 4 mESL) in the 20–30 ka period. The misfit region with 95% (2σ) confidence from the minimum misfit (red dot) is denoted by the grey shading (misfit values below 5.99) [*Press et al.*, 1992]. The VM5a structure, used in the previous part, is denoted in blue. All six results show that GRACE is not able to distinguish between different lithosphere thicknesses in the Barents Sea.

To enable the ICE-5G model to pass the GRACE criterion, a smaller upper mantle viscosity is required to account for the large ice volume. The smaller upper mantle viscosity will result in a faster rebound and results in smaller current gravity change, due to the fact that most of the relaxation has finished. The opposite effect is seen with the minimum ice volume model nn44901, where a larger upper mantle viscosity is needed, such that there is still enough current gravity change present. The best fitting rheology for the late deglaciation model (maximum overall ice mass) and ICE-5G has an upper mantle viscosity of 4×10^{20} Pa s. This is similar to the regional upper mantle viscosity estimate of *Steffen and Kaufmann* [2005]. The early deglaciation ice models

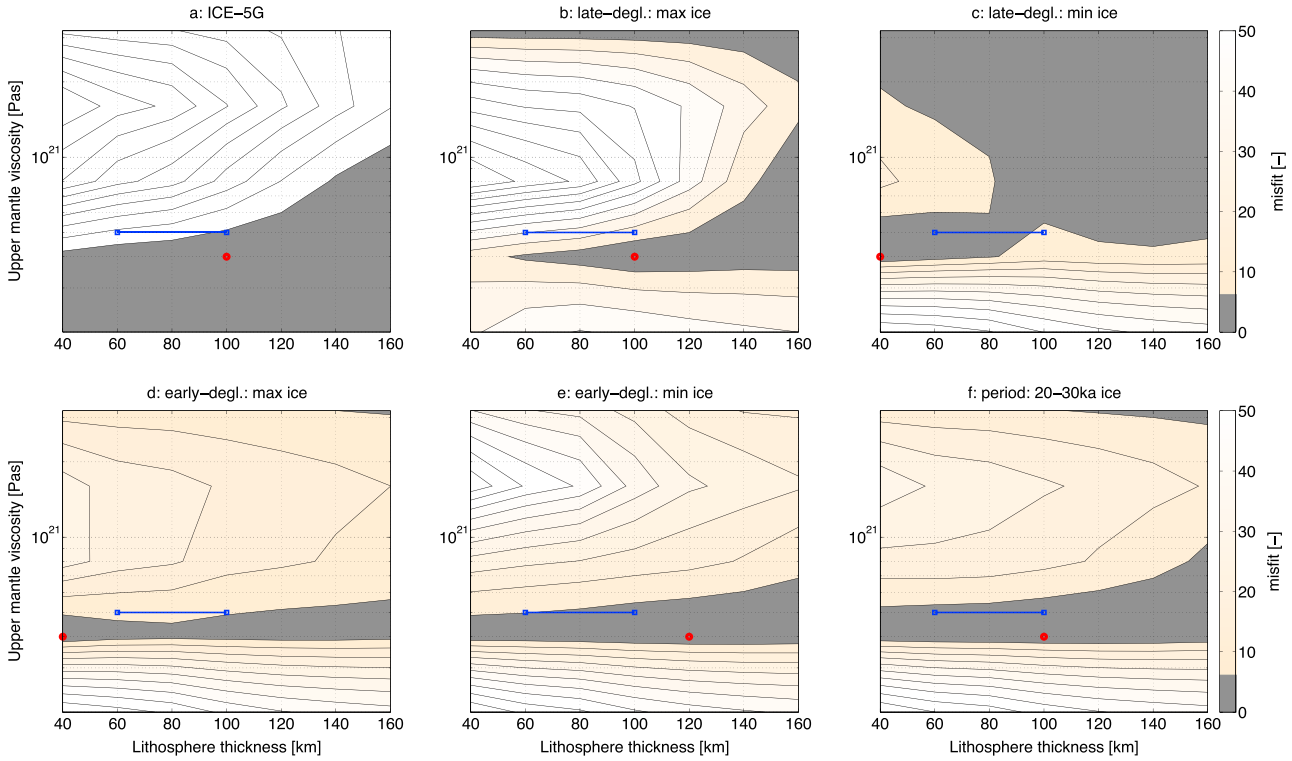

Figure 3. The misfit values from the comparison of the GIA model with different ice-loading histories to the corrected GRACE observations. The red dot denotes the minimum misfit with a confidence region (2σ) illustrated by the grey area. The different ice-loading histories are (a) ICE-5G (global ice model); (b) ice model nn44195 (maximum ice volume, late deglaciation); (c) ice model nn44901 (minimum ice volume, late deglaciation); (d) ice model nn54867 (maximum ice volume, early deglaciation); (e) ice model nn55778 (large ice volume at 20–30 ka, early deglaciation); and (f) ice model nn56597 (minimum ice volume, early deglaciation). The VM5a viscosity profile is illustrated by the blue dots.

show a more consistent behavior. Here best upper mantle viscosities have a clear lower limit of 4×10^{20} Pa s. Overall, the ice model with maximum ice mass during LGM (nn54867) constrains the upper mantle viscosity to be between 4 and 5×10^{20} Pa s.

6. Concluding Remarks

The increasing time span of the GRACE gravity change observations now permits the use of these observations for GIA studies of the Barents Sea region. After filtering and correcting for present-day ice melt, GRACE data show a positive gravity change where GIA is expected. Estimates of the systematic error introduced by correcting for present-day ice melt and for formal error demonstrate that the positive signal is significant.

The global ice-loading models ICE-5G and ICE-6G overestimate the observed gravity change in the Barents Sea region. The regional ice-loading models, which contain less ice mass, predict a gravity rate that is closer to the GRACE-derived result. The late deglaciation chronology models mostly overestimate the observed gravity change. GRACE is therefore able to add new constraints to the ice mass histories:

1. Late deglaciation ice-loading models with less than 5.1 mESL during LGM pass the GRACE criterion.
2. Early deglaciation ice-loading models with more than 5.2 mESL during LGM pass the GRACE criterion.

Our rheological sensitivity study indicates that the late deglaciation ice models can be made to fit the GRACE data by lowering the upper mantle viscosity to 4×10^{20} Pa s, similar rheological changes are needed for ICE-5G. The early deglaciation chronology ice sheet models result in a clear lower limit of the upper mantle viscosity of 4×10^{20} Pa s.

To explain the inferred 120–130 m sea level rise since LGM, the total volume of the LGM ice sheets in global models needs to increase. Our results show that it is difficult for the Barents Sea to be a candidate for missing ice. The regional ice models that better fit the GRACE gravity change contain approximately 2 mESL less overall ice mass in the Barents Sea region than the global ICE-5G and ICE-6G models. GRACE observations constrain

the maximum ice thickness to be thinner than predicted by these ice-loading histories with the VM5a Earth rheology. Otherwise the upper mantle viscosity needs to be lowered with respect to the VM5a viscosity profile that was used to infer ice thickness from RSL constraints. ICE-5G and ICE-6G regional RSL fits would then need to be reexamined. In summary, the GRACE data distinguish between ice-loading histories that fit the RSL and GPS uplift data and, therefore, offer new constraint on the deglacial evolution of the Barents Sea region.

Acknowledgments

The authors would like to thank Ernst Schrama for providing the mascon mass change estimates in this study. We thank Anna L.C. Hughes, Richard Gyllencreutz, Øystein S. Lohne, Jan Mangerud and John Inge-Svendsen for the provision of unpublished data from the DATED project. We also thank Halfdan Kierulf, and Holger Steffen for the provision of the updated and expanded set of observed vertical velocities and guidance on their uncertainties. Finally, we like to thank Volker Klemann and an anonymous reviewer for their thorough review of the manuscript. Funding for this study was provided by the Netherlands Organisation for Scientific Research (NWO). This is also a contribution to the project Eurasian Ice Sheet and Climate Interaction (EISCLIM) financially supported by the Research Council of Norway (project 229788/E10). Data and models can be requested from the corresponding author.

The Editor thanks Volker Klemann and an anonymous reviewer for their assistance in evaluating this paper.

References

Argus, D. F., and W. R. Peltier (2010), Constraining models of postglacial rebound using space geodesy: A detailed assessment of model ICE-5G (VM2) and its relatives, *Geophys. J. Int.*, *181*, 697–723.

Austermann, J., J. X. Mitrovica, K. Latychev, and G. A. Milne (2013), Barbados-based estimate of ice volume at Last Glacial Maximum affected by subducted plate, *Nat. Geosci.*, *6*, 553–557.

Bettadpur, S. (2003), Level-2 gravity field product user handbook, *The GRACE Project*, Jet Propulsion Lab., Pasadena, Calif.

Briggs, R., D. Pollard, and L. Tarasov (2014), A data-constrained large ensemble analysis of Antarctica evolution since the Emian, *Quat. Sci. Rev.*, *103*, 91–115, doi:10.1016/j.quascirev.2014.09.003.

Cheng, M., B. D. Tapley, and J. C. Ries (2013), Deceleration in the Earth's oblateness, *J. Geophys. Res. Solid Earth*, *118*, 740–747, doi:10.1002/jgrb.50058.

Clark, P. U., and L. Tarasov (2014), Closing the sea level budget at the Last Glacial Maximum, *Proc. Natl. Acad. Sci. U.S.A. Commentary*, *111*, 15861–15862.

Greff-Lefftz, M., L. Métivier, and J. Besse (2010), Dynamic mantle density heterogenities and global geodetic observables, *Geophys. J. Int.*, *180*, 1080–1094.

Grosswald, M. G. (1998), Late-Weichselian ice sheet in Arctic and Pacific Siberia, *Quat. Int.*, *45–46*, 3–18.

Hughes, A. L. C., J. Mangerud, R. Gyllencreutz, J. I. Svendsen, and Ø. S. Lohne (2014), Evolution of the Eurasian Ice Sheets during the last deglaciation (25-10 kyr), Abstract PP51D-1165 paper presented at 2014 Fall Meeting, AGU, San Francisco, Calif., 13–19 Dec.

Ivins, E., T. S. James, J. Wahr, E. J. O. Schrama, F. W. Landerer, and K. M. Simon (2013), Antarctic contribution to sea level rise observed by GRACE with improved GIA correction, *J. Geophys. Res. Solid Earth*, *118*, 3126–3141, doi:10.1002/jgrb.50208.

Jacob, T., J. Wahr, W. T. Pfeffer, and S. Swenson (2012), Recent contributions of glaciers and ice caps to sea level rise, *Nature*, *482*, 514–518.

Kaufmann, G. (1997), The onset of Pleistocene glaciation in the Barents Sea: Implications for glacial isostatic adjustment, *Geophys. J. Int.*, *131*, 281–292.

Kendall, R. A., J. X. Mitrovica, and G. A. Milne (2005), On post-glacial sea level—II. Numerical formulation and comparative results on spherically symmetric models, *Geophys. J. Int.*, *161*(3), 679–706.

Kierulf, H. P., H. Steffen, M. J. R. Simpson, M. Lidberg, P. Wu, and H. Wang (2014), A GPS velocity field for Fennoscandia and a consistent comparison to glacial isostatic adjustment models, *J. Geophys. Res. Solid Earth*, *119*, 66134–6629, doi:10.1002/2013JB010889.

Lambeck, K. (1996), Limits on the areal extent of the Barents Sea ice sheet in late Weichselian time, *Global Planet. Change*, *12*, 41–51.

Lambert, A., N. Courtier, and T. James (2006), Long-term monitoring by absolute gravimetry: Tides to postglacial rebound, *J. Geodyn.*, *41*, 307–317.

Mangerud, J., V. Astakhov, and J.-I. Svendsen (2002), The extent of the Barents-Kara ice sheet during the Last Glacial Maximum, *Quat. Sci. Rev.*, *21*, 111–119.

Mitrovica, J. X., and W. R. Peltier (1991), On postglacial geoid subsidence over the equatorial oceans, *J. Geophys. Res.*, *96*(B12), 20,053–20,071.

Moholdt, G., C. Nuth, J. O. Hagen, and J. Kohler (2010), Recent elevation changes of Svalbard glaciers derived from ICESat laser altimetry, *Remote Sens. Environ.*, *114*, 2756–2767.

Moholdt, G., B. Wouters, and A. S. Gardner (2012), Recent mass changes of glaciers in the Russian High Arctic, *Geophys. Res. Lett.*, *39*, L10502, doi:10.1029/2012GL051466.

Nuth, C., G. Moholdt, J. Kohler, J. O. Hagen, and A. Kääb (2010), Svalbard glacier elevation changes and contribution to sea level rise, *J. Geophys. Res.*, *115*, F01008, doi:10.1029/2008JF001223.

Peltier, W. (2004), Global glacial isostasy and the surface of the ice-age Earth: The ICE-5G (VM2) model and GRACE, *Annu. Rev. Earth Planet. Sci.*, *32*(1), 111–149.

Peltier, W., and R. Drummond (2008), Rheological stratification of the lithosphere: A direct inference based upon the geodetically observed pattern of the glacial isostatic adjustment of the North American continent, *Geophys. Res. Lett.*, *35*, L16314, doi:10.1029/2008GL034586.

Peltier, W., and R. Fairbanks (2006), Global glacial ice volume and Last Glacial Maximum duration from an extended Barbados sea level record, *Quat. Sci. Rev.*, *25*, 3322–3337.

Press, W., S. Teukolsky, W. Vetterling, and B. Flannery (1992), Numerical recipes in FORTRAN; The Art of scientific computing.

Ritzmann, O., and J. I. Faleide (2009), The crust and mantle lithosphere in the Barents Sea/Kara Sea region, *Tectonophysics*, *470*, 89–104.

Rodell, M., et al. (2004), The global land data assimilation system, *Bull. Am. Meteorol. Soc.*, *85*, 381–394.

Root, B. C., J. Ebbing, W. van der Wal, P. Novák, and L. Vermeersen (2015), Glacial isostatic adjustment in the static gravity field of Fennoscandia, *J. Geophys. Res. Solid Earth*, *120*, 503–518, doi:10.1002/2014JB0115084.

Schmidt, P., B. Lund, J.-O. Näslund, and J. Fastook (2014), Comparing a thermo-mechanical Weichselian ice sheet reconstruction to reconstructions based on the sea level equation: Aspects of ice configurations and glacial isostatic adjustment, *Solid Earth*, *5*, 371–388.

Schrama, E. J. O., B. Wouters, and R. Rietbroek (2014), A mascon approach to assess ice sheet and glacier mass balances and their uncertainties from GRACE data, *J. Geophys. Res. Solid Earth*, *119*, 6048–6066, doi:10.1002/2013JB010923.

Shepherd, A., et al. (2012), A reconciled estimate of ice-sheet mass balance, *Science*, *338*(6111), 1183–1189.

Steffen, H., and G. Kaufmann (2005), Glacial isostatic adjustment of Scandinavia and northwestern Europe and the radial viscosity structure of the Earth's mantle, *Geophys. J. Int.*, *163*, 801–812.

Steffen, H., H. Denker, and J. Muller (2008), Glacial isostatic adjustment in Fennoscandia from GRACE data and comparison with geodynamical models, *J. Geodyn.*, *46*, 155–164.

Svendsen, J. I., et al. (2004), Late quaternary ice sheet history of northern Eurasia, *Quat. Sci. Rev.*, *23*(11–13), 1229–1271.

Tamisiea, M., J. Mitrovica, and J. Davis (2007), GRACE gravity data constrain ancient ice geometries and continental dynamics over Laurentia, *Science*, *316*, 881–883.

Tarasov, L., A. S. Dyke, M. N. Radford, and W. R. Peltier (2012), A data-calibrated distribution of deglacial chronologies for the North American ice complex from glaciological modeling, *Earth Planet. Sci. Lett.*, *315–316*, 30–40.

van der Wal, W., A. Braun, P. Wu, and M. G. Sideris (2009), Prediction of decadal slope changes in Canada by glacial isostatic adjustment modelling, *Can. J. Earth Sci.*, *46*(1), 587–595.
van der Wal, W., E. Kurtenbach, J. Kusche, and B. Vermeersen (2011), Radial and tangential gravity rates from GRACE in areas of glacial isostatic adjustment, *Geophys. J. Int.*, *187*, 797–812.
Vermeersen, L., and R. Sabadini (1997), A new class of stratified viscoelastic models by analytical techniques, *Geophys. J. Int.*, *129*, 531–570.
Wahr, J., M. Molenaar, and F. Bryan (1998), Time variability of the Earth's gravity field: Hydrological and oceanic effects and their possible detection using GRACE, *J. Geophys. Res.*, *103*(B12), 30,205–30,229.
Wahr, J., S. Swenson, V. Zlotnicki, and I. Velicogna (2004), Time-variable gravity from GRACE: First results, *Geophys. Res. Lett.*, *31*, L11501, doi:10.1029/2004GL019779.
Whitehouse, P. L., M. J. Bentley, and A. M. L. Brocq (2012), A deglacial model for Antarctica: Geological constraints and glaciological modelling as a basis for a new model of Antarctic glacial isostatic adjustment, *Quat. Sci. Rev.*, *32*, 1–24.
Wu, P., and W. R. Peltier (1982), Viscous gravitational relaxation, *Geophys. J. R. Astron. Soc.*, *70*(1), 435–485.